Evaluation of dental implant stability using ultrasonic characterization and multifractal analysis

I. SCALA[a], G. ROSI[a], V.-H. NGUYEN[a], S. NAILI[a], R. VAYRON[a], G. HAIAT[a], S. SEURET[b] and S. JAFFARD[b]

a. Université Paris-Est, Laboratoire Modélisation et Simulation Multi Echelle, MSME UMR 8208 CNRS, 61, Avenue du Général de Gaulle, 94010 Créteil, France; e-mail: ilaria.scala@u-pec.fr, giuseppe.rosi@u-pec.fr, vu-hieu.nguyen@u-pec.fr, naili@u-pec.fr, romain.vayron@u-pec.fr, haiat@u-pec.fr

b. Université Paris-Est, LAMA UMR 8050, UPEM, UPEC, CNRS, 61, Avenue du Général de Gaulle, 94010 Créteil, France; e-mail: seuret@u-pec.fr, jaffard@u-pec.fr

Résumé :

L'évaluation de la stabilité d'un implant est une tâche importante pour les dentistes. La stabilité à long terme d'un implant dentaire dépend de la qualité du tissu osseux entourant l'implant. Les conditions limites à l'interface os-implant ainsi que la complexité du tissu osseux néoformé (un milieu complexe, anisotrope, poreux-viscoélastique en constant remodelage) rendent difficiles cette évaluation. Plusieurs paramètres affectent les stabilités primaire et secondaire, tels que la qualité, la densité et la quantité d'os en contact avec l'implant. Dans ce cadre, les techniques basées sur les ultrasons se sont avérées efficaces pour l'estimation des stabilités primaire et secondaire. La réponse ultrasonore de l'implant dépend de la microstructure, des propriétés mécaniques et de la géométrie du système os-implant. Les principales interrogations sont i) identifier la signature spécifique laissée par ces propriétés sur le signal et ii) extraire l'information à partir du signal. Des modèles mécaniques avancés décrivant l'échantillon cible associées à d'importantes techniques de traitement des signaux peuvent être utilisées.

L'objectif de ce travail est de traiter les signaux ultrasonores obtenus á partir de notre dispositif sous différentes conditions en utilisant des techniques basées sur l'analyse multifractale.

Des simulations *via* la méthode par éléments finis ont été réalisées pour reproduire différents types de stabilité d'implant (avec un dévissage progressif). L'avantage de la simulation numérique par rapport aux expériences est la possibilité de réaliser de manière contrôlée des analyses de sensibilité par rapport à des paramètres comme la densité et la rigidité de l'os. Les résultats expérimentaux (pour l'os mouillé et l'os sec) ainsi que numériques (en considérant une étude paramétrique en faisant varier la fréquence et la densité de l'os trabéculaire) sont comparés, et ensuite analysés *via* des outils de traitement du signal basés sur les méthodes d'analyse multifractale.

Dans ce contexte, l'analyse multifractale a comme but de décrire les propriétés d'échelle du signal. L'objectif est d'extraire des paramètres significatifs capable de caractériser la composition et/ou les propriétés microstructurales de l'interface os-implant (invariance d'échelle). En regardant les valeurs moyennes des fonctions de structure par rapport au dévissage (de l'implant), une corrélation peut être remarquée.

Abstract:

The evaluation of implant stability is an important task for dentists. The long-term stability of a dental implant is dependent on the quality of bone tissue surrounding it. In this context, difficulties are mostly due to the complexity of newly formed bone tissue (a complex, anisotropic, porous-viscoelastic medium in constant remodeling) but also to the boundary conditions at the bone-implant interphase. In particular, multiple parameters affect primary and secondary stability, as bone quality, bone density or amount of bone in contact with the implant.
In this framework, ultrasound based techniques have already been proven to be effective in the qualitative and quantitative evaluation of primary and secondary stability of dental implants. The ultrasonic response of the implant depends on the microstructure, mechanical properties and geometry of the bone-implant system. Major questions are: how each of these properties leaves a specific signature on the signal, and how the information can be extracted. One must conceive advanced mechanical models describing the target sample associated with relevant signal processing techniques.
The purpose of this work is to process ultrasonic signals obtained with our ultrasonic device in different environments using signal processing based on multifractal analysis.
Implants with different stabilities, obtained by suitably unscrewing the dental implant, are simulated using a finite element software. The advantage of numerical simulations with respect to experiments is that a sensitivity analysis with respect to parameters such as bone density and stiffness can be performed in a controlled manner. Both experimental (for wet bone and dry bone) and numerical (a parametric study varying the frequency and the trabecular bone density has been considered) results are compared, and then analyzed by signal processing tools based on multifractal methods. In this context, the aim of multifractal analysis is to describe signal scale properties. The aim is to extract relevant parameters able to characterize the composition and/or the microstructural properties of bone-implant inter-phase (scale invariance). By looking at the mean values of the structure functions to the level of unscrewing (of the implant), a correlation can be observed.

Mots clefs : implant stability, multifractal analysis, numerical simulations, wave propagation

1 Introduction

With the aim of surgical success, the evaluation of implant stability is important. The implant stability can be considered as divided into two stages: primary or mechanical stability (reached during the implant placement) and secondary or biological stability (after bone remodeling). The long-term anchorage of the implant is critically dependent on the peri-implant bone, *e.g.* on the bone remodelling at the interface bone-implant [6], which leads to changes in the bone mechanical properties [9]. In this context, difficulties are due to bone (a complex, anisotropic, porous-viscoelastic and in constant remodeling medium), its multiscale and time-evolving nature [5], and its boundary conditions at the interphase bone-implant. While ultrasonic methods are already been proven to be effectively used in quantifying dental implant stability, see *e.g.* [10, 11, 12, 13], simple signal processing techniques have been employed. In this framework, ultrasound wave propagation methods applied to dental implants (which act as wave-guides) are arousing an increasing interest. Moreover, parameters such as bone structure, geometry or mechanical properties are rather complex to handle *in vivo*, as they vary in parallel; therefore

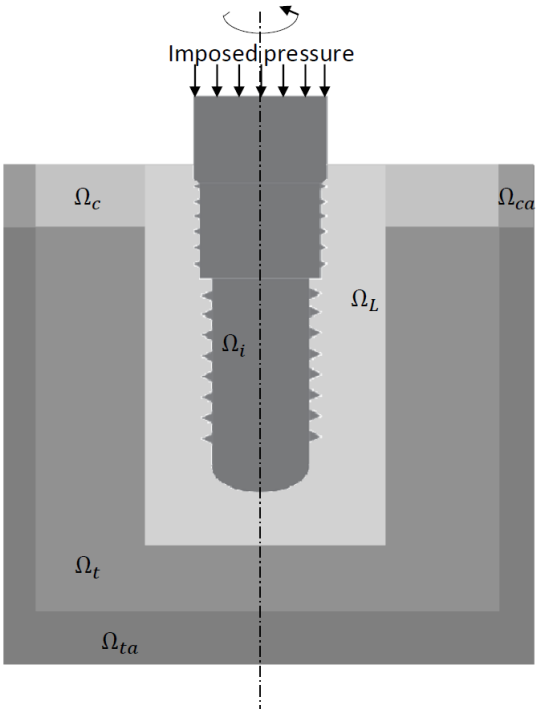

Figure 1: Cross-section view of the 3-D axisymmetric geometrical configuration used in the numerical simulations. The domains are denoted with a subscript corresponding to the variable material (Ω_L), the trabecular bone (Ω_t), the cortical bone (Ω_c), the implant (Ω_i), and the absorbing layers associated to trabecular and cortical bone (Ω_{ta} and Ω_{ca}, respectively).

modeling as a resource to discriminate them in the ultrasonic response is becoming more and more important.

Here, numerical studies, based on finite element model on the wave propagation into a dental implant inserted in bone, are carried out. The signals obtained are complex and difficult to interpret since they come from multiple reflections at the interface bone-implant. This encourages to use advanced techniques based on multifractal analysis. Actually, fractal and/or multifractal analysis has already been proposed as a possible approach for similar irregular and complex biological data [4, 7, 8].

With the aim of simplifying calculations, an axisymmetric geometry has been considered.

2 Geometrical configuration and Finite Element (FE) analysis

According to the configuration shown in Figure 1, where a perfect symmetry with respect to the implant central axis can be appreciated, an axisymmetric situation has been assumed. On the emerging surface of the implant a contact planar 10 MHz transducer is placed. The bone model is realized as a double-layer structure composed by a cortical bone 1 mm thick and an half-space of trabecular bone. The geometrical configuration shown in Figure 1 corresponds to the titanium dental implant commercialized by Implants Diffusion International (IDI1240, IDI, Montreuil, France), with a length of $L = 11.5$ mm and a diameter of $D = 4$ mm. Moreover, a specific healing abutment is inserted in the upper part of the implant in order to avoid tissue formation inside. This configuration with the implant totally inserted in the bone specimen is the typical clinical set-up. The region between implant surface mature bone tissue, where we can have bone tissue or water, is the peri-prosthetic layer, named Ω_L. Here, we will assume that all

the considered media exhibit isotropic homogeneous mechanical properties, and also that volume forces are neglected.

The aforementioned contact transducer, located on the upper emerging surface of the specimen, generate a signal correspondent to a time pulse uniform pressure; its temporal function can be expressed as follows:

$$p(t) = Ae^{-4(f_c t-1)^2 \sin(2\pi f_c t)}, \tag{1}$$

where A is the amplitude, f_c is the pulse central frequency and t is the time.

The discretization of the equations, leads to a transient linear elastic problem, a complete description of which can be found in [12]. Additionally, we can obtain the output signal frequency rf with a space average of the pressure defined in Eq. (1). The signal envelope has been considered in a first try [10, 11] to extract informations from the complex signal with which we deal. The analysis technique used in [10], which gives a quantitative indicator I, is useful to check the consistency between numerical simulations and experiences. This indicator is based on the temporal variation of the signal amplitude and is defined as:

$$I = \sum_{i=1}^{N} S(it_0) \tag{2}$$

where N designates the samples number, t_0 is the sampling rate and $S(t)$ the signal envelope. As an example, a recorded signal plot from numerical test is shown in Figure 2. Note that in this work we go a step further by considering that the recorded signal came from multiple reflections at the interface bone-implant, thus we attend to extract more information by a multi-scale analysis.

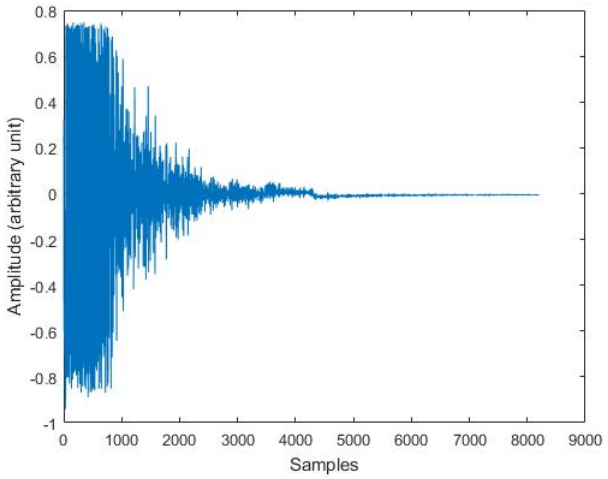

Figure 2: Example of an output signal obtained with our ultrasonic device.

3 Signal processing and multifractal analysis

In this work, multifractal tools are employed to extract relevant information from the scaling properties of signals either derived from experimental and numerical data. The hope is to characterize the composition and/or the micro-structural properties of bone implant inter-phase. Multifractal analysis consists in determining *scaling functions* associated with the data and discussing their relevance using classification methods or model selection.

3.1 Wavelet basis

Starting with the functions $\phi(x)$ and $\psi(x)$ (regular and well localized), an orthonormal wavelet basis on $L^2(\mathbb{R})$ is defined as the set of functions $\phi(x-k)$ and $2^{j/2}\psi(2^j x-k)$, where $j \geq 0$ and $k \in \mathbb{Z}$. The basis is "r-smooth" if $\phi(x)$ and $\psi(x)$) have derivatives up to order r which have fast decay. We denote by $c_{j,k}$ and c_j the *wavelets coefficients* on the function f

$$c_{j,k} = 2^j \int_{\mathbb{R}} f(x)\psi(2^j x-k)dx, \qquad c_k = \int_{\mathbb{R}} f(x)\phi(x-k)dx. \tag{3}$$

These coefficients give informations on the oscillations of f in the neighborhood of the dyadic interval $\lambda(=\lambda(j,k)) := \left[k2^{-j},(k+1)2^{-j}\right)$, which leads to a more compact notation, that is $c_\lambda = c_{j,k}$ and $\psi_\lambda(x) = \psi(2^j x-k)$. This kind of indexation is useful because the wavelet ψ_λ is fundamentally located near the dyadic interval λ. Furthermore, we denote by Λ_j is the set of dyadic intervals λ of width 2^{-j} . A L^1 normalization for wavelet coefficients is used because it is more natural in order to express scale invariance relations.

3.2 Wavelets structure functions

The wavelet structure functions of f are defined by

$$\forall j \in \mathbb{N}, \quad \forall p > 0, \qquad S_f(p,j) = 2^{-j} \sum_{\lambda \in \Lambda_j} |c_\lambda|^p . \tag{4}$$

Multifractal analysis usually proposes to use classification tools based on log-log plot regressions of structure functions (the so-called *scaling functions*, see [1, 2]). However, in our case, log-log plots do not display a clear scaling-invariance behavior (see Figures 3a-3b-4). Therefore it seems more relevant to base classification directly on the structure functions (note that a similar idea was followed in [3] for old photographic papers). One possibility is to consider quantities which are used in the wavelet characterization of homogeneous Besov spaces $\dot{B}_p^{0,p}(\mathbb{R})$ (the space $\dot{B}_p^{0,p}(\mathbb{R})$ is closely related with the $L^p(\mathbb{R})$ space, see [1, 2]). Recall that the wavelet characterization of these spaces implies that, if wavelets are smooth enough (which we assume), then

$$\| f \|^p_{\dot{B}_p^{0,p}(\mathbb{R})} \quad \sim \quad \sum_j 2^{-j} \sum_{\lambda \in \Lambda_j} |c_\lambda|^p = \sum_j S_f(p,j). \tag{5}$$

We propose to perform classification on these quantities, see Fig. 5a-5b-5c.

4 Results and discussion

We used the Wavelet Leader and Bootstrap [14, 15] based MultiFractal analysis (WLBMF) toolbox. We applied this analysis to both experimental (wet and dry bone) and numerical simulations. As already said, the hope is to extract relevant parameters able to characterize the composition and/or the micro-structural properties of bone-implant inter-phase (scale invariance properties). Our data came from output signals recorded from two configurations, that are the "dry" and the "wet" (to simulate buccal condition) bone conditions. For each configuration, a progressive unscrewing of 2π-rad of the dental implant is considered. The rotations performed are 4 to 5, depending on the specimen.

A first look at the signal output (see Figure 2) suggest that it can be thought as divided into two parts :

a first one, where there is a constant trend because of a saturation of the amplitude, and a second part (after ~ 1000 samples) with a decreasing exponential trend. Thus, the first 1000 samples of the signal can be cut off.

In Figures 3a-3b-4 the structure functions of the signals are shown for different levels of stability. With this in mind, several observations can be made:

- small scales (*e.g.* $j < 3$) does not include any informations, in fact they are constant for each case considered;
- for large scales (*e.g.* $j > 6$) it is remarkable that simulations differ from experiences. The additional informations presented by the experiences is not reported by simulations because they do not contain anything more about stability (that is what we look for in this work);
- therefore, it is reasonable to take into account only a part of the signal (*e.g.* $j \in [3, 6]$);
- the p-value has been chosen equal to 1 because small ps lead to more stable computations.

Thus, by looking at Figures 3a-3b-4, inside the aforementioned window, experiences and simulation are coherent. We estimate that the different trend that is visible for low scales (j>6) is mostly due to the fact that the specimen used in experiments has finite dimensions, while the numerical model is supposed to be unbounded. Indeed, the information carried by this part of the structure function it is not relevant for the characterization of the bone implant interface.

Moreover, following the classification method described in section 3.2, we perform a linear regression on the mean values of the structure functions (see Figures 5a-5b-5c) in function of the unscrewing. A correlation can be clearly observed. In the figures presented, the minimal stability case (that is the implant totally unscrewed in air) have been neglected because it is not interesting for our analysis. In the upper left of each figures the R-squared coefficient is indicated. This coefficient is higher for the "dry bone" case (see Figure 5a) than the others (see Figures 5b-5c). This is the only configuration that exhibits a linear trend. Indeed, the "wet bone" configuration, as well as the simulations, show more a quadratic correlation than a linear one. Moreover, these later cases represent a more realistic situation.

Finally, in order to validate the multi-fractal analysis with respect to the results presented in [10, 11, 12, 13], we compare the results obtained for the same simulation (with $\rho_t = 1170\ \mathrm{kg/m^3}$ and $f_c = 10$ MHz), for the indicator I, computed following Equation 2, and the mean value of the structure functions. This comparison is presented in Figures 6a and 6b. In both curves, a quadratic trend is evidenced as well as the coherence between them.

In addition, from Figure 5a to Figure 6b a saturation for low level of stability (*i.e.* for increasing level of unscrewing) can be appreciated.

5 Conclusion

This study highlights, by comparing experimental and numerical results, and analyzing them by signal processing with multifractal methods, the possibility to explore and exploit the multiscale structure of the signal for evaluating implant stability. In addition, using multifractal analysis, it has been evidenced that the mean values of the structure functions are coherent with the indicator used in [10, 11, 12, 13].

To sum up, the finite element analysis of a 3D axisymmetric configuration has been considered and some preliminary results from multifractal analysis have been carried out. In a further work, the introduction of

"multifractality" from a geometrical point of view (*e.g.* geometrical configurations like Menger sponges and Koch iterations) as well as to find a model which contains "multifractal elements" are envisaged in order to exploit the real potential of multifractal analysis [1, 3, 2]) by using tools as the scaling exponent, the multifractal spectrum [7] or the log-cumulants.

Acknowledgments

This project was supported by the Université Paris-Est through the PEPS program (15R03051A- MET-CARMAT). G.R. wishes to thank the Faculté de Sciences et Technologie de l'Université Paris-Est Créteil for the financial support.

References

[1] P. Abry, S. Jaffard, H. Wendt, Irregularities and scaling in signal and image processing: multifractal analysis, in: *Benoit Mandelbrot: A Life in Many Dimensions*, WORLD SCIENTIFIC, Chapter 3, 31–116, 2015.

[2] P. Abry, S. Jaffard, H. Wendt, A bridge between geometric measure theory and signal processing: Multifractal analysis, in: *Operator-Related Function Theory and Time-Frequency Analysis*, Springer, 1–56, 2015.

[3] P. Abry, S. G. Roux, H. Wendt, P. Messier, A. G. Klein, N. Tremblay, P. Borgnat and S. Jaffard, B. Vedel, J. Coddington, L. A. Daffner, Multiscale Anisotropic Texture Analysis and Classification of Photographic Prints: Art scholarship meets image processing algorithms, *IEEE Signal Processing Magazine*, Vol. **32**, N. **4**, 18–27, 2015.

[4] D. Chappard, M.-F. Baslé, E. Legrand, M. Audran, Trabecular bone microarchitecture: a review, *Morphologie*, Vol. **92**, N. **299**, 162–170, 2008.

[5] H. M. Frost, Bone's mechanostat: A 2003 update, *The Anatomical Record Part A: Discoveries in Molecular, Cellular, and Evolutionary Biology*, Vol. **89**, N. **6**, 1081–1101, 2003.

[6] Y. Gabet, D. Kohavi, R. Voide, T. L. Mueller, R. Müller, I. Bab, Endosseous implant anchorage is critically dependent on mechanostructural determinants of peri-implant bone trabeculae, *Journal of Bone and Mineral Research*, Vol. **25**, N. **3**, 575–583, 2010.

[7] Z. Gao, W. Hong, Y. Xu, T. Zhang, Z. Song, J. Liu, Osteoporosis Diagnosis Based on the Multifractal Spectrum Features of Micro-CT Images and C4.5 Decision Tree, *Pervasive Computing Signal Processing and Applications (PCSPA), 2010 First International Conference on IEEE*, 1043-1047,2010.

[8] W. G. Geraets, P. F. Van der Stelt, Dentomaxillofacial Radiology, *Journal of Bone and Mineral Research*, Vol. **29**, N. **3**, 144–153, 2000.

[9] G. Luo, A. M. Sadegh, H. Alexander, W. Jaffe, D. Scott, S. C. Cowin, The effect of surface roughness on the stress adaptation of trabecular architecture around a cylindrical implant, *Journal of biomechanics*, Vol. **32**, N. **3**, 275–284, 1999.

[10] R. Vayron, P. Karasinski, V. Mathieu, A. Michel, D. Loriot, G. Richard, G. Lambert, G. Haïat, Variation of the ultrasonic response of a dental implant embedded in tricalcium silicate-based cement under cyclic loading, *Journal of biomechanics*, Vol. **46**, N. **6**, 1162–1168, 2013.

[11] R. Vayron, V. Mathieu, A. Michel, G. Haïat, Assessment of in vitro dental implant primary stability using an ultrasonic method, *Ultrasound in medicine & biology*, Vol. **40**, N. **12**, 2885–2894, 2014.

[12] R. Vayron, V.-H. Nguyen, R. Bosc, S. Naili, G. Haïat, Finite element simulation of ultrasonic wave propagation in a dental implant for biomechanical stability assessment, *Biomechanics and modeling in mechanobiology*, Vol. **14**, N. **5**, 1021–1032, 2015.

[13] R. Vayron, V.-H. Nguyen, R. Bosc, S. Naili, G. Haïat, Assessment of the biomechanical stability of a dental implant with quantitative ultrasound: A three-dimensional finite element study, *The Journal of the Acoustical Society of America*, Vol. **139**, N. **2**, 773–780, 2016.

[14] H. Wendt, P. Abry, S. Jaffard, Bootstrap for empirical multifractal analysis, *IEEE signal processing magazine*, Vol. **24**, N. **4**, 38–48, 2007.

[15] H. Wendt, S. G. Roux, S. Jaffard, P. Abry, Wavelet leaders and bootstrap for multifractal analysis of images, *Signal Processing*, Vol. **89**, N. **6**, 1100–1114, 2009.

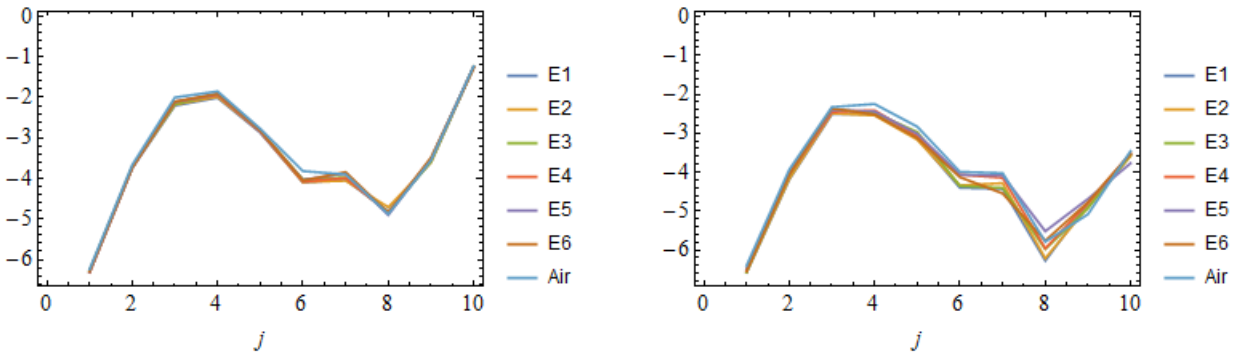

(a) Dry bone

(b) Wet bone

Figure 3: (Colors online). Wavelet structure functions (DWT) (for $p = 1$) performed on experimental data obtained from two different configurations. On the right a legend for the curves is presented, where for several steps progressive insertion of the dental implant into bone a distinction can be made: "$E1$" represents the implant fully inserted in bone tissue, "Ei" ($i = 1, ..., n$) the implant unscrewed of $2\times$iπ-rad, and "Air" the implant located in the air (which means that there isn't bone tissue around the implant).

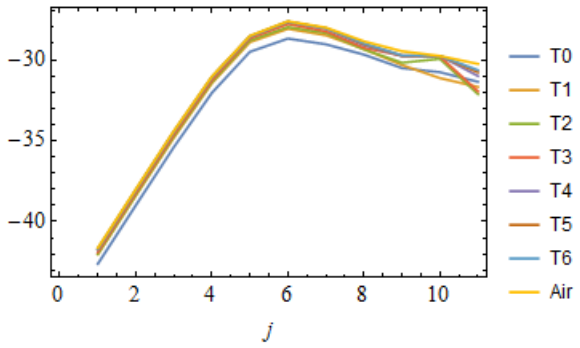

Figure 4: (Colors online). Wavelet structure functions (DWT) (for $p = 1$) performed on numerical data. On the right a legend for the curves is presented, where for several steps progressive insertion of the dental implant into bone a distinction can be made: "$T0$" represents the implant fully inserted in bone tissue, "Ti" ($i = 1, ..., n$) the implant unscrewed of $2\times$iπ-rad, and "Air" the implant located in the air (which means that there isn't bone tissue around the implant).

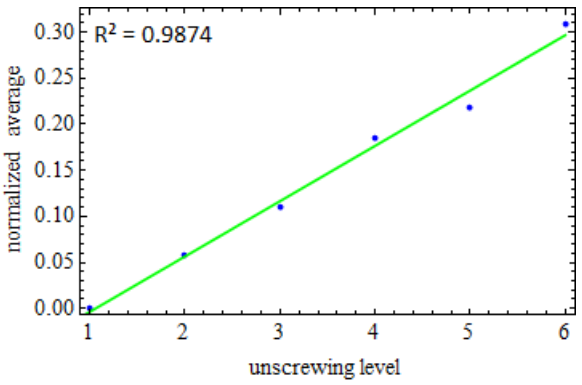

(a) Dry bone

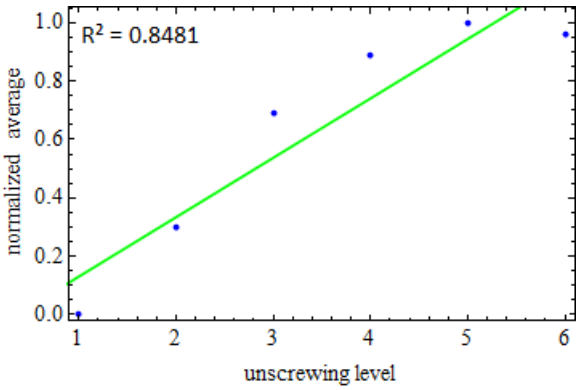

(b) Wet bone

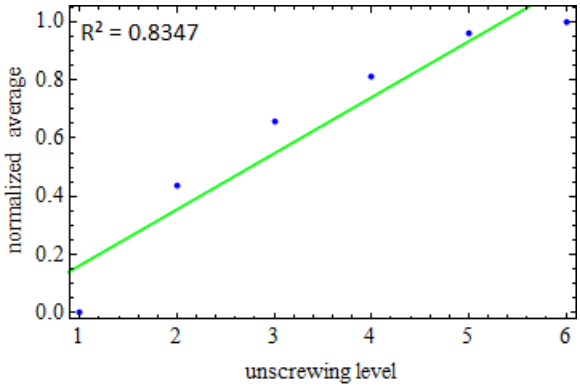

(c) Simulation.

Figure 5: (Colors online). Mean values of the structure functions (for $p = 1$) to the increasing level of unscrewing for all the configurations studied: a) dry bone, b) wet bone and c) simulation.

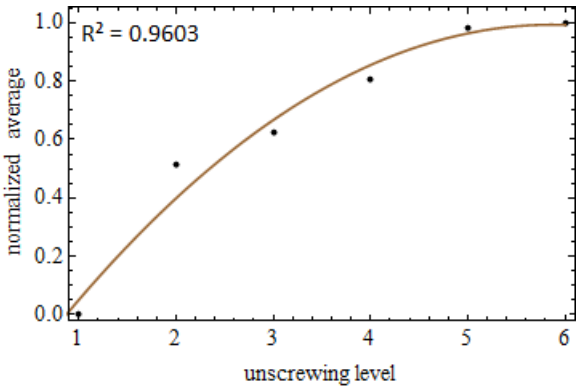

(a)

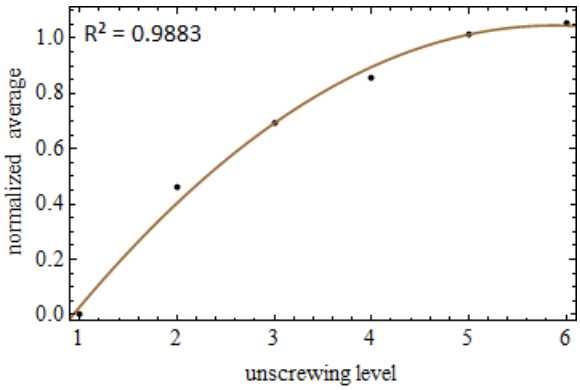

(b)

Figure 6: (Colors online). Quadratic regression for a) the indicator I and b) for the mean values of the structure functions (for $p = 1$).